

Anomalous optical diffraction by a phase grating induced by a local field effect in semiconductor quantum dots

Yasuyoshi Mitsumori,^{1,*} Tetsuya Watanuki,¹ Yuki Sato,¹ Keiichi Edamatsu,¹ Kouichi Akahane,² and Naokatsu Yamamoto²

¹*Research Institute of Electrical Communication, Tohoku University, Sendai 980-8577, Japan*

²*National Institute of Information and Communications Technology, Tokyo 184-8795, Japan*

(Received 10 August 2016; revised manuscript received 3 March 2017; published 3 April 2017)

We demonstrate the use of laser-induced phase gratings to control the emission characteristics of self-assembled semiconductor quantum dots. The microscopic Coulomb interaction between the photoinduced charge densities in a dot, referred to as the local field effect, affects the macroscopic optical properties of a dot ensemble even with inhomogeneous broadening, and forms a phase grating by spatially modulating the exciton resonant frequency. In the low excitation regime, the diffracted light intensity (observed using photon echoes) gradually rose with time delay—a result very different from the conventional instantaneous response to pulse excitation. With increasing excitation intensity, the response of the diffracted signal became more immediate and exhibited a biexponential decay. The change in the temporal profile can be systematically explained by analyzing the dynamics of the phase grating. Our findings suggest an optical switching mechanism using this intrinsic property of semiconductor quantum dots.

DOI: [10.1103/PhysRevB.95.155301](https://doi.org/10.1103/PhysRevB.95.155301)

I. INTRODUCTION

A grating with a spatially periodic structure diffracts light into different propagation directions. There are two kinds of gratings: amplitude gratings and phase gratings. An amplitude grating realizes light diffraction by periodically modulating the amplitude of light passing through or reflected by the grating [1]. On the other hand, a phase grating (such as a surface relief grating) imprints a spatially periodic phase shift onto a light field [1]. Therefore a phase grating can diffract light into various directions. The diffracted light intensity depends on the phase contrast [1]. When two laser pulses with different wave vectors are applied to a material, the refractive index and the absorption coefficient are spatially periodically modulated, forming a grating, referred to as a laser-induced grating [2–4]. The diffracted light is usually observed as transient grating signals [5–8], photon echoes [9–15], and four-wave-mixing signals [8,16–20]. As illustrated in Fig. 1(a), in the case of an ensemble of electronic states, such as two-level systems, the coherent interaction of the polarization excited by the first pulse with wave vector \mathbf{k}_1 and the light field of the second pulse with \mathbf{k}_2 spatially modulates the population difference $\rho_D = \rho_{ee} - \rho_{gg}$ between the excited state ρ_{ee} and the ground state ρ_{gg} , inducing a population grating $\rho_D \propto \cos(\mathbf{k}_2 - \mathbf{k}_1) \cdot \mathbf{x}$ [4,11], as shown in Fig. 1(c). In the framework of nonlinear optics [11], the optical diffraction at resonance by the population grating is described by the electric field caused by the nonlinear polarization, which is generated by the interaction between the light incident on the population grating and ρ_D . Therefore the electric field has the same spatial distribution as the population grating. In this sense, the population grating behaves as an amplitude grating [7]. In semiconductor quantum dots (QDs), electronic states, i.e., excitons, lead to an additional effect, because anisotropically shaped QDs show exciton doublet fine structure in their photo-luminescence spectrum [21], demonstrating that the electron-hole exchange interaction inside the single

excitons renormalizes the exciton resonance itself [22,23]. The exchange interaction is a Coulomb interaction between photoinduced charge densities [22–26], which are connected with the polarization densities, as $\rho(\mathbf{r}) = -\nabla \cdot \mathbf{p}(\mathbf{r})$. In a QD, as illustrated in Fig. 1(a), the microscopic charge densities spatially distributed in the single exciton interact with each other. In other words, the local field generated by $\rho(\mathbf{r})$ interacts with $\mathbf{p}(\mathbf{r}')$, which composes the excitonic polarization. Therefore the Coulomb interaction in the single exciton dynamically shifts the resonant frequency ω_r of the exciton itself with a change in the polarization. This is known as a local field effect (LFE) occurring within QDs [15,27–30]. According to the LFE theory [28,29], the shift of ω_r simply depends on the exciton population difference ρ_D . Therefore, as shown in Fig. 1(c), the population grating spatially periodically modulates the resonant frequency $\omega_r \propto \cos(\mathbf{k}_2 - \mathbf{k}_1) \cdot \mathbf{x}$, indicating that the time-evolution of the modulated frequency induces a phase grating. The phase contrast m is proportional to time t , as $m \propto \omega_r t$; the relationship is the same as that in frequency modulation and phase modulation. Therefore the propagation direction and the light intensity diffracted by the phase grating are expected to vary anomalously with time. Anomalous light diffraction in localized exciton systems in a single quantum well has been reported as an experimental signature of local fields [13]. However, in well-defined conventional QDs, such anomalous diffraction has not yet been observed. In addition, the dynamic phase grating induced by the resonant frequency shift of electronic states has never been discussed before.

In this paper, we report the observation of a laser-induced dynamic phase grating in self-assembled QDs. We observed the light diffraction as a two-pulse photon echo (PE) response, which showed strong dependence on the excitation intensity. The diffraction by the phase grating induced by the LFE is discussed using simple calculations, which reproduce the observations quantitatively, as well as qualitatively. Both the observations and the calculations indicate that the dominant grating for the diffraction shifts from the phase to the population grating with increasing excitation intensity. We also analyze the higher-order PE signal originating from the phase

*mitsumori@riec.tohoku.ac.jp

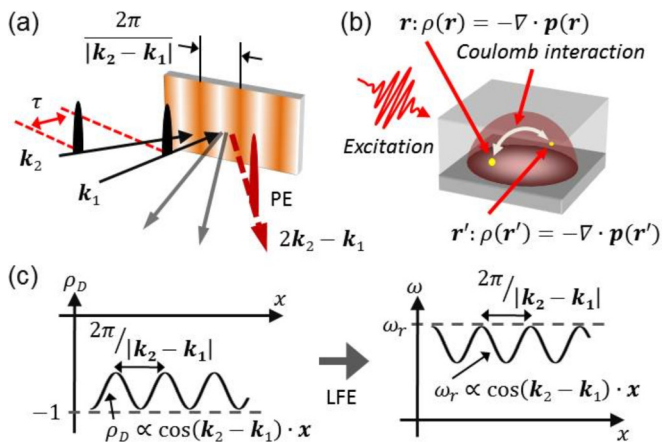


FIG. 1. (a) Illustration of the grating induced by the two-laser-pulse excitation and the diffraction of the second pulse as a PE signal along $2\mathbf{k}_2 - \mathbf{k}_1$ in the reflection geometry. (b) Schematic drawing of the Coulomb interaction of the photoinduced charge densities in a single exciton in a QD. (c) Illustration of a population grating for homogeneous QD systems with the same resonant frequency and a change in ω_r induced by the LFE before (dashed line) and after (solid line) the excitation.

grating. Our experimental findings and simple calculations demonstrate novel optical coherent transients based on QDs, and indicate that the microscopic Coulomb interaction in a QD strongly affects the macroscopic optical property of the QD ensemble even with inhomogeneous broadening.

II. SAMPLE AND EXPERIMENTAL METHODS

The sample used in this work was a single layer of self-assembled QDs fabricated by molecular beam epitaxy on a GaAs (311)*B* substrate. After the 360-nm growth of $\text{Al}_{0.17}\text{Ga}_{0.83}\text{As}$ as a buffer layer, $\text{In}_{0.4}\text{Al}_{0.1}\text{Ga}_{0.5}\text{As}$ QDs were grown by the Stranski-Krastanov growth mode, and then a 200-nm $\text{Al}_{0.17}\text{Ga}_{0.83}\text{As}$ layer was grown as a capped layer. The QDs had a dome shape and their density was $\sim 1.1 \times 10^{10} \text{ cm}^{-2}$. The photoluminescence (PL) peak at 3.5 K was located at 1.565 eV, and the inhomogeneous broadening arising from the size distribution was ~ 40 meV. A more detailed characterization can be found in Ref. [15].

The experiment was carried out by means of a two-pulse PE technique. The light source was a mode-locked Ti:Sapphire laser with a repetition rate of 76 MHz. The temporal duration and spectral width of the laser pulses were ~ 1.4 ps and ~ 0.5 meV, respectively. The center photon energy was set to the PL peak at 1.565 eV. The laser pulses were divided into two beams, which were parallel linear-polarized and focused on the same spot on the sample. The beam spot had a Gaussian profile with a full width at the half maximum of ~ 65 μm . The PE signal along $2\mathbf{k}_2 - \mathbf{k}_1$ in the reflection geometry, as illustrated in Fig. 1(a), was fed into a monochromator. The PE intensity was recorded as a function of the time delay τ between the first and second pulses.

III. RESULTS AND DISCUSSION

Figure 2(a) shows the PE intensity detected as a function of τ for the various intensities of the first pulse $I_1 = I_0, 3I_0,$

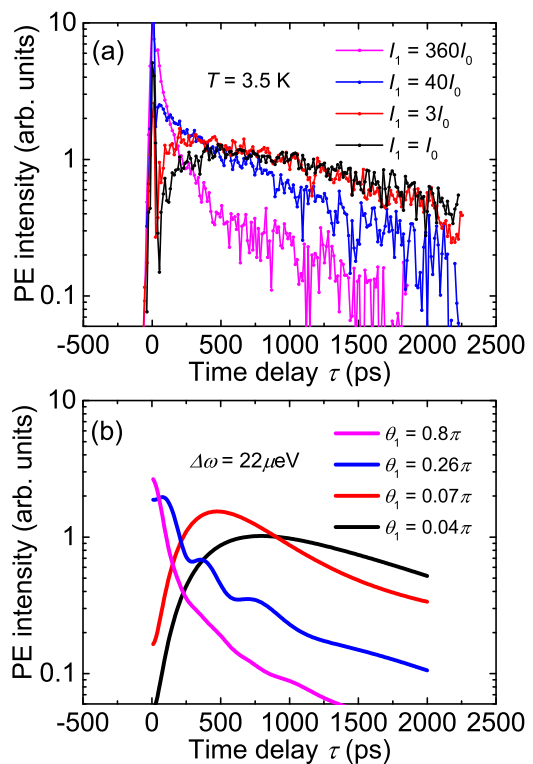


FIG. 2. (a) PE intensity detected as a function of τ for various I_1 when $I_2 = 360I_0$, where $I_0 \sim 8 \text{ nJ cm}^{-2}$ per pulse. (b) Calculated PE intensity as a function of τ when $\theta_2 = 0.8\pi$.

$40I_0$, and $360I_0$, when the second pulse intensity I_2 was set to $I_2 = 360I_0$, where $I_0 \sim 8 \text{ nJ/cm}^2/\text{pulse}$. In all scans, a large peak at zero time delay was observed. We attribute the large peak to the GaAs substrate because the carriers in bulk crystals show a fast dephasing time [12]. In the $I_1 = I_0$ scan in Fig. 2(a), the PE intensity rose until $\tau \sim 600$ ps, and then began to decay exponentially. With increasing I_1 , the peak position moved toward zero time delay. At the highest I_1 , the temporal profile showed an instantaneous response to the excitation, followed by a biexponential decay. The decay time constant of the signal in the longer τ regime was slightly shorter with increasing I_1 . In the weak excitation regime, the decay time was estimated to be ~ 750 ps, while it was ~ 650 ps for higher I_1 . These two values indicated that the dephasing time T_2 could be evaluated to be $T_2 = 2.6 \sim 3.0$ ns in our excitation range. We estimated the relation between I_1 and the corresponding pulse area θ_1 using the Rabi oscillations in our previous report [15], which has used the same sample and experimental setup. The excitation intensities $I_1 = I_0, 3I_0, 40I_0$, and $360I_0$ could be calibrated to be $\theta_1 \sim 0.04\pi, 0.07\pi, 0.26\pi$, and 0.8π at the center of the beam spot, respectively, and the pulse area of the second pulse could be estimated as $\theta_2 \sim 0.8\pi$.

As alluded to before, the observed PE response exhibits a unique dependence on τ . In the framework of LFE theory [28,29], the Coulomb effect in a QD takes part in the optical nonlinearity by shifting the exciton resonance $\omega_r = \omega_0 - \Delta\omega\rho_D$, where ω_0 denotes the resonant frequency without LFE, and $\Delta\omega$ represents the depolarization shift, which is given by $\Delta\omega = N_x\mu^2/\hbar\epsilon_h V$ using the dipole moment

μ , the volume V , the depolarization tensor N_x of a QD, and the dielectric constant of the host material ϵ_h [27–29]. The subscript x in N_x represents the polarization direction.

First, we discuss the experimental results using a perturbative treatment, which successfully explains the role of the phase grating induced by the LFE in the PE response for small θ_1 , although we used large θ_2 in our experiment. For high excitations, we use numerical calculations as will be discussed later. We start with homogeneous QD systems by assuming that QDs are spatially distributed with uniformity and that $\rho_D(t < 0) = -1$, i.e., the exciton in each QD has the same resonant frequency $\omega_r^{<0} = \omega_0 + \Delta\omega$ before the excitation by the first pulse at $t = 0$. The population grating induced by the two-pulse excitation can be written by $\rho_D(t > \tau) = \theta_1\theta_2 \cos \varphi - 1$ in the low excitation regime [11]. φ indicates the phase difference between the two incident pulses $\varphi = (\mathbf{k}_2 - \mathbf{k}_1) \cdot \mathbf{x} + \delta\omega\tau$, where \mathbf{x} and $\delta\omega$ denote the location of a QD and a detuning term $\delta\omega = \omega_r - \omega_L$ using the laser frequency ω_L , respectively. The resonant frequency after the second pulse changes to $\omega_r^{>\tau} = \omega_0 + \Delta\omega - \Delta\omega\theta_1\theta_2 \cos \varphi$. Therefore the LFE gives a spatially periodic frequency shift to the exciton resonance through the population grating.

When we view the oscillations $e^{-i\omega_r^{>\tau}(t-\tau)}$ from the rotating frame of $\omega_r^{<0} = \omega_0 + \Delta\omega$, the time-evolution of the frequency modulation forms a phase grating as $\phi_g = -\Delta\omega\theta_1\theta_2 \cos \varphi \times (t - \tau)$. Supposing that the PE signal appears at $t = 2\tau$, the phase contrast is proportional to τ . Therefore, as shown in Fig. 3, the low phase contrast at $\tau \sim 0$ creates small amplitude oscillations with a period $\Lambda = 2\pi / |\mathbf{k}_2 - \mathbf{k}_1|$ in the imaginary part of the phase factor $\text{Im}(e^{-i\phi_g})$, which gives extremely small diffraction efficiency. Then, the amplitude of $\text{Im}(e^{-i\phi_g})$ gradually increases with τ , which enhances the diffraction efficiency leading to a rise in the diffracted signal. When the contrast is close to $\sim\pi$, the oscillations with a period Λ in $\text{Im}(e^{-i\phi_g})$ attain their maximum amplitude, which realizes maximum diffraction of the second pulse into $2\mathbf{k}_2 - \mathbf{k}_1$. On the other hand, the real part begins to oscillate with a period $\Lambda/2$, which diffracts into $3\mathbf{k}_2 - 2\mathbf{k}_1$. A further increase in the contrast decreases the component with a period Λ , while giving an increase in the oscillations with real and imaginary

spatial periods of $\Lambda/2$ and $\Lambda/3$, respectively. Therefore the phase grating changes the diffraction direction of the second pulse as a function of τ .

The above qualitative analyses can be theoretically described using the Jacobi-Anger expansion as

$$e^{-i\phi_g} = \sum_n i^n J_n(\Delta\omega\theta_1\theta_2(t-\tau)) e^{in\varphi}, \quad (1)$$

where J_n represents the Bessel function of the first kind. Using perturbation theory [11], the nonlinear polarization for the diffraction in the rotating frame can be written as

$$P_{NL} \propto \rho_D(t > \tau) \theta_2 e^{ik_2 \cdot \mathbf{x} - i\phi_g}. \quad (2)$$

Therefore the diffraction efficiency along $(n+1)\mathbf{k}_2 - n\mathbf{k}_1$ is given by J_n , which depends on time.

Let us focus on the diffraction along $2\mathbf{k}_2 - \mathbf{k}_1$. When we use arbitrary pulse areas for the excitation, $\rho_D(t > \tau)$ in Eq. (2) can be rewritten by $\rho_D(t > \tau) = \sin \theta_1 \sin \theta_2 \cos \varphi - \cos \theta_1 \cos \theta_2$. Therefore there are two components to the signal. One is the signal directly diffracted by the population grating, which corresponds to the diffraction by an amplitude grating and yields a conventional PE signal. The signal field amplitude is proportional to the contrast of the population grating, i.e., $\sin \theta_1 \sin \theta_2$. The other is generated by the first-order diffraction given by the phase grating. For the phase grating, the signal field depends on the spatial mean value of the population $\langle \rho_D(t > \tau) \rangle$ in the population grating because the phase grating signal is generated by the term independent of the wave vector in $\rho_D(t > \tau)$, i.e., $-\cos \theta_1 \cos \theta_2$, which corresponds to $\langle \rho_D(t > \tau) \rangle$.

We can find the PE signal at $t = 2\tau$ as a δ -function-like signal by integrating over the linewidth of the inhomogeneous broadening, which is assumed to be infinity for simplicity. The signal intensity is calculated as

$$I_{PE} \propto |i\theta_1\theta_2^2 J_0(\Delta\omega\theta_1\theta_2\tau) - \theta_2 J_1(\Delta\omega\theta_1\theta_2\tau)|^2. \quad (3)$$

The first term represents the diffraction by the population grating and the second term results from the phase grating. Because small θ_1 gives $J_0 \rightarrow 1$ and $J_1 \rightarrow \Delta\omega\theta_1\theta_2\tau/2$, the dominant signal arises from the phase grating, when $\Delta\omega\tau \gg 1$. Thus the phase grating induced by the LFE is the cause of the signal at short times τ . At longer τ , the PE response is affected by a dephasing process, which shows an exponential decay. When θ_1 is increased, the rise time is faster, which moves the signal peak to shorter τ . We note here that the phase grating induced by the LFE is important for the optical response even in the third-order optical nonlinearity, when the dephasing rate is negligibly smaller than $\Delta\omega$. On the other hand, for the larger dephasing rate, the phase grating is masked by the linewidth. Therefore the resonant frequency shift can be neglected in the nonlinear optical response, as can be seen in quantum wells [18,19,31,32] and dense two-level systems [20,32].

For large θ_1 , we calculated the PE response using the Bloch equation for the LFE [28] by a nonperturbative treatment. Figure 2(b) shows the calculated PE response along $2\mathbf{k}_2 - \mathbf{k}_1$ for various θ_1 when $\theta_2 = 0.8\pi$ and $\hbar\Delta\omega = 22 \mu\text{eV}$. The amount of $\hbar\Delta\omega$ has been obtained in our previous report [15]. In the calculation, we assumed a δ -function-like pulse for the excitation, which gives the condition $\mu E_i(t)/\hbar \gg \delta\omega, \Delta\omega$, where $E_i(t)$ is field amplitude of the i -th pulse. With this

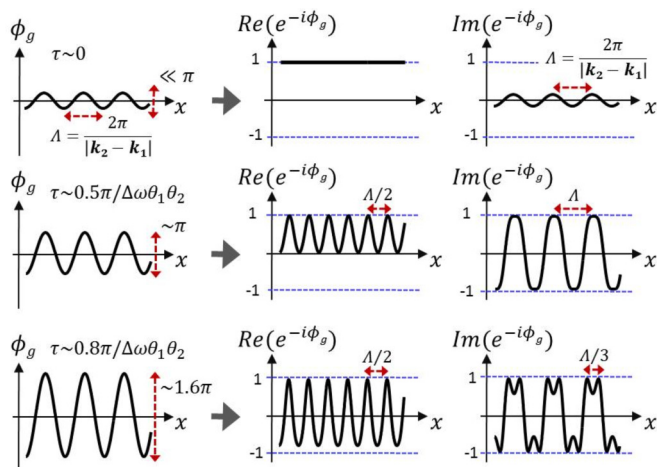


FIG. 3. (Left) Illustration of the phase grating ϕ_g induced by the LFE at $t = 2\tau$. (Right) The real and imaginary parts of the phase factor $e^{-i\phi_g}$.

assumption, we could analytically calculate the polarization along $2\mathbf{k}_2 - \mathbf{k}_1$ in presence of the LFE, when the arbitrary pulse areas were used for the excitations. We introduced the effects of $T_2 = 2.8$ ns, which is the mean value of T_2 in our excitation range, and the lifetime $T_1 = 2.0$ ns [15] by adding damping terms to the Bloch equation. In our measurement, the monochromator with a narrow entrance slit spatially extracted the approximately one-dimensional component from the focused image of the signal on the slit. Therefore we numerically integrated the PE intensity over the one-dimensional component of the signal image when the excitation beam spot had a Gaussian profile, which modifies a coherent optical response of QDs [14]. θ_1 and θ_2 in Fig. 2(b) represent the pulse areas of the first and second pulses at the center of the excitation beam spot, respectively.

The calculated curves, as a whole, reproduce the change in the experimental profile using the experimentally estimated values of $\theta_{1,2}$. Therefore the calculations agree well quantitatively, as well as qualitatively. In the perturbative treatment, the temporal profile is described by $J_{1,2}(\Delta\omega\theta_1\theta_2\tau)$. Therefore large $\theta_{1,2}$ shorten the oscillation period of $J_{1,2}$, implying that the temporal profile has the form of a damped oscillation. However, a Gaussian beam profile gives the oscillations of $J_{1,2}$ different periods depending on the location of the QD in the beam spot. Thus the summation of curves with different periods over the signal image greatly reduces the visibility of the oscillations in the temporal profile. In addition, at longer τ , the population grating decays with the energy relaxation, which decreases the phase contrast, i.e., $\phi_g \rightarrow 0$. Therefore the optical response of the QDs is close to that of two-level systems with increasing τ , which also contributes to the reduction in the visibility and gives an exponential decay reflecting the dephasing process.

With increasing θ_1 , the contrast of the population grating is higher, while $(\rho_D(t > \tau)) \rightarrow 0$. Therefore the population grating dominantly diffracts the second pulse, which generates the PE signal immediately after the excitation. However, the phase grating induced by the LFE takes part in the diffraction by the population grating as the diffraction efficiency of J_0 , which can be seen in Eq. (3). The highest I_1 in the experiment gives an extremely short oscillation period to J_0 , which makes the slope of the beginning of the oscillations much steeper than that of the exponential decay caused by the dephasing process. Therefore the PE intensity rapidly decreases during an initial transient period of length ~ 500 ps, after which it settles into a slower exponential decay, resulting in the overall biexponential decay profile seen in the high excitation regime.

In Fig. 2(b), the calculated curve for $\theta_1 = 0.26\pi$ shows small oscillations, which originate from the oscillations of $J_{0,1}$ imperfectly-eliminated by the beam profile. We infer that the calculated curve would be more suitably reproduced by introducing a distribution of $\Delta\omega$, which reduces the visibility by dispersing the oscillation periods. However, we speculate that the distribution is not trivial, because $\Delta\omega$ depends on μ , V , and N_x [27–29]. Therefore we expect that a detailed analysis of the distribution and an advanced theoretical treatment are needed for a more accurate reproduction. Nevertheless, the qualitative agreement with the observations and our simple calculations indicates that the observed change in the PE response can be attributed to the phase grating induced by the LFE.

Next, we discuss the higher-order PE signal along $(n+1)\mathbf{k}_2 - n\mathbf{k}_1$. Equation (1) indicates that the phase grating gives the n th-order phase difference $n\delta\omega\tau$ arising from the detuning, together with $n(\mathbf{k}_2 - \mathbf{k}_1)$. Therefore the n th-order signal can be found at $t = (n+1)\tau$ by integrating over the inhomogeneous broadening. In addition, Eqs. (1) and (2) indicate that the higher-order signal does not contain a J_0 component. Thus the temporal profile is expected to show a rise in the signal following the excitation even under high excitations. A change in the rise time depending on the excitation intensity is, therefore, to be expected.

We briefly mention the spectrum measurement of the exciton resonant frequency shift induced by the LFE using single-dot spectroscopies. Experiments using a continuous wave (CW) laser generally give a high-resolution spectrum. In the LFE, the high excitation in resonance with the exciton effectively increases ρ_D , and significantly shifts the resonance. However, the high optical field generated by a CW laser gives rise to a stationary dressed state, which dominates the spectrum shape [33–35]. Therefore it is better to use transient techniques for measuring the spectrum after pump irradiation at high powers, because the transient method is solely affected by the LFE. In addition, $\Delta\omega$ is proportional to N_x . The tightly-localized isotropic wave functions of the excitons, like in spherical QDs, produce a large value of N_x [29]. On the other hand, disklike QDs give $N_x \sim 0$ for the in-plane polarization direction parallel to the sample surface [27], yielding no resonance shift, and $N_x \sim 1$ for the direction normal to the surface [27]. Cavity systems are not suitable because the radiative line-broadening prevents the observation of the small resonance shift.

Finally, our findings here provide a novel scheme for optical switching devices using an intrinsic property of QDs. The phase grating induced by the LFE, as discussed above, dynamically diffracts light into various directions, suggesting that the propagation direction of a light field can be manipulated by actively controlling the phase contrast. We expect that such a device will be realized using techniques of coherent manipulation for quantum states, such as Rabi oscillations [13–15, 36–38] and phase-locked pulse pairs [38–40], which can directly manipulate the population difference shifting the exciton resonance frequency.

IV. CONCLUSION

In conclusion, we observed an anomalous PE response in the InAlGaAs/AlGaAs QDs. The temporal profile of the PE signal strongly depended on the excitation intensity. The change in the temporal profile could be systematically explained by analyzing the phase grating induced by the LFE. The microscopic Coulomb interaction in a QD strongly affects the macroscopic optical property of a QD ensemble even with inhomogeneous broadening. We also discussed the higher-order PE signal diffracted by the phase grating. Our findings are important for further development of optical devices based on QDs.

ACKNOWLEDGMENTS

This work was supported in part by Japan Society for the Promotion of Science, KAKENHI Grants No. 20740168 and

No. 23340083. We thank Y. Ogawa of Joetsu University of Education and M. Sadgrove of Tohoku University for helpful

discussions. Y.M. acknowledges support from the M. Ishida foundation.

-
- [1] J. W. Goodman, *Introduction to Fourier Optics*, 3rd ed. (Roberts & Company Publishers, Englewood, Colorado, 2005).
- [2] H. J. Eichler, *Opt. Acta* **24**, 631 (1977).
- [3] A. V. Jena and H. E. Lessing, *Opt. Quantum. Electron.* **11**, 419 (1979).
- [4] H. J. Eichler, P. Günter, and D. W. Pohl, *Laser-Induced Dynamic Gratings* (Springer-Verlag, Berlin, 1986).
- [5] H. Eichler, G. Salje, and H. Stahl, *J. Appl. Phys.* **44**, 5383 (1973).
- [6] D. W. Pohl, S. E. Schwarz, and V. Irniger, *Phys. Rev. Lett.* **31**, 32 (1973).
- [7] K. A. Nelson, R. Casalegno, R. J. D. Miller, and M. D. Fayer, *J. Chem. Phys.* **77**, 1144 (1982).
- [8] L. Schultheis, J. Kuhl, A. Honold, and C. W. Tu, *Phys. Rev. Lett.* **57**, 1797 (1986).
- [9] N. A. Kurnit, I. D. Abella, and S. R. Hartmann, *Phys. Rev. Lett.* **13**, 567 (1964).
- [10] I. D. Abella, N. A. Kurnit, and S. R. Hartmann, *Phys. Rev.* **141**, 391 (1966).
- [11] T. Yajima and Y. Taira, *J. Phys. Soc. Jpn.* **47**, 1620 (1979).
- [12] P. C. Becker, H. L. Fragnito, C. H. Brito Cruz, R. L. Fork, J. E. Cunningham, J. E. Henry, and C. V. Shank, *Phys. Rev. Lett.* **61**, 1647 (1988).
- [13] Y. Mitsumori, A. Hasegawa, M. Sasaki, H. Maruki, and F. Minami, *Phys. Rev. B* **71**, 233305 (2005).
- [14] M. Kujiraoka, J. Ishi-Hayase, K. Akahane, N. Yamamoto, K. Ema, and M. Sasaki, *Phys. status solidi (a)* **206**, 952 (2009).
- [15] K. Asakura, Y. Mitsumori, H. Kosaka, K. Edamatsu, K. Akahane, N. Yamamoto, M. Sasaki, and N. Ohtani, *Phys. Rev. B* **87**, 241301 (2013).
- [16] R. L. Carman, R. Y. Chiao, and P. L. Kelley, *Phys. Rev. Lett.* **17**, 1281 (1966).
- [17] L. Schultheis, J. Kuhl, A. Honold, and C. W. Tu, *Phys. Rev. Lett.* **57**, 1635 (1986).
- [18] H. Wang, K. Ferrio, D. G. Steel, Y. Z. Hu, R. Binder, and S. W. Koch, *Phys. Rev. Lett.* **71**, 1261 (1993).
- [19] H. Wang, K. B. Ferrio, D. G. Steel, P. R. Berman, Y. Z. Hu, R. Binder, and S. W. Koch, *Phys. Rev. A* **49**, R1551(R) (1994).
- [20] S. T. Cundiff, *Laser Phys.* **12**, 1073 (2002).
- [21] D. Gammon, E. S. Snow, B. V. Shanabrook, D. S. Katzer, and D. Park, *Phys. Rev. Lett.* **76**, 3005 (1996).
- [22] T. Takagahara, *Phys. Rev. B* **47**, 4569 (1993).
- [23] T. Takagahara, *Phys. Rev. B* **62**, 16840 (2000).
- [24] K. Cho, *J. Phys. Soc. Jpn.* **68**, 683 (1999).
- [25] H. Ajiki and K. Cho, *Phys. Rev. B* **62**, 7402 (2000).
- [26] H. Ajiki, T. Tsuji, K. Kawano, and K. Cho, *Phys. Rev. B* **66**, 245322 (2002).
- [27] G. Y. Slepyan, S. A. Maksimenko, A. Hoffmann, and D. Bimberg, *Phys. Rev. A* **66**, 063804 (2002).
- [28] G. Y. Slepyan, A. Magyarov, S. A. Maksimenko, A. Hoffmann, and D. Bimberg, *Phys. Rev. B* **70**, 045320 (2004).
- [29] G. Y. Slepyan, A. Magyarov, S. A. Maksimenko, and A. Hoffmann, *Phys. Rev. B* **76**, 195328 (2007).
- [30] G. Gligorić, A. Maluckov, L. Hadžievski, G. Y. Slepyan, and B. A. Malomed, *Phys. Rev. B* **88**, 155329 (2013).
- [31] M. Wegener, D. S. Chemla, S. Schmitt-Rink, and W. Schäfer, *Phys. Rev. A* **42**, 5675 (1990).
- [32] J. M. Shacklette and S. T. Cundiff, *J. Opt. Soc. Am. B* **20**, 764 (2003).
- [33] X. Xu, B. Sun, P. R. Berman, D. G. Steel, A. S. Bracker, D. Gammon, and L. J. Sham, *Science* **317**, 929 (2007).
- [34] A. N. Vamivakas, Y. Zhao, C.-Y. Lu, and M. Atatüre, *Nat. Phys.* **5**, 198 (2009).
- [35] E. B. Flagg, A. Muller, J. W. Robertson, S. Founta, D. G. Deppe, W. M. M. Xiao, G. J. Salamo, and C. K. Shih, *Nat. Phys.* **5**, 203 (2009).
- [36] T. H. Stievater, X. Li, D. G. Steel, D. Gammon, D. S. Katzer, D. Park, C. Piermarocchi, and L. J. Sham, *Phys. Rev. Lett.* **87**, 133603 (2001).
- [37] P. Borri, W. Langbein, S. Schneider, U. Woggon, R. L. Sellin, D. Ouyang, and D. Bimberg, *Phys. Rev. B* **66**, 081306 (2002).
- [38] H. Kamada, H. Gotoh, J. Temmyo, T. Takagahara, and H. Ando, *Phys. Rev. Lett.* **87**, 246401 (2001).
- [39] A. P. Heberle, J. J. Baumberg, and K. Köhler, *Phys. Rev. Lett.* **75**, 2598 (1995).
- [40] N. H. Bonadeo, J. Erland, D. Gammon, D. Park, D. S. Katzer, and D. G. Steel, *Science* **282**, 1473 (1998).